RSC Advances

This is an *Accepted Manuscript*, which has been through the Royal Society of Chemistry peer review process and has been accepted for publication.

Accepted Manuscripts are published online shortly after acceptance, before technical editing, formatting and proof reading. Using this free service, authors can make their results available to the community, in citable form, before we publish the edited article. This *Accepted Manuscript* will be replaced by the edited, formatted and paginated article as soon as this is available.

You can find more information about *Accepted Manuscripts* in the Information for Authors.

Please note that technical editing may introduce minor changes to the text and/or graphics, which may alter content. The journal's standard Terms & Conditions and the Ethical guidelines still apply. In no event shall the Royal Society of Chemistry be held responsible for any errors or omissions in this *Accepted Manuscript* or any consequences arising from the use of any information it contains.

ROYAL SOCIETY OF CHEMISTRY

www.rsc.org/advances

Cite this: DOI: 10.1039/c0xx00000x

www.rsc.org/xxxxxx

COMMUNICATION

Mechanism study of Li^+ insertion into titania nanotubes

Nareerat Plylahan,[a] A. Demoulin, C. Lebouin, Philippe Knauth[a,b,c] and Thierry Djenizian[*a,b,c]

Received (in XXX, XXX) Xth XXXXXXXXX 20XX, Accepted Xth XXXXXXXXX 20XX
DOI: 10.1039/b000000x

The Li^+ insertion into anatase titania nanotubes (TiO_2nts) employing PEO-based polymer electrolyte has been studied by cyclic voltammetry and chronoamperometry. The study shows that the Li^+ storage in the anatase is dominated by the bulk diffusion (into the lattice) and the increasing contribution of the pseudo-capacitive effect with faster kinetics We also report that the chemical diffusion of Li^+ in self-organized titania nanotubes is around 2×10^{-16} cm^2 s^{-1} suggesting that the use of a solid electrolyte does not alter the charge transport in the nanostructured electrode.

Titania nanotubes (TiO_2nts) have been extensively studied as a negative electrode for lithium-ion batteries (LIBs). Thanks to their nanotubular structure, TiO_2nts show a suitable morphology to fabricate 3D lithium-ion microbatteries[1] for nomadic applications. All-solid-state microbatteries are preferable for the safety concerns and the ease of the fabrication. For these reasons, highly flammable organic liquid electrolyte must be avoided and replaced by solid or polymer electrolytes. Polymer electrolyte such as poly(ethylene oxide) (PEO) – based polymer shows interesting properties such as good ionic conductivity[2,3], electrochemical stability[4], thermal stability[5] and flexibility. Recently, we have reported the fabrication of half and full cells based on TiO_2nts as negative and lithium-bis-(trifluormethanesulfonyl)-imide (LiTFSI) dissolved in PEO-based polymer electrolyte.[6–8] These cells exhibit good performances e.g. good capacity and high stability upon cycling. However, the mechanism of the Li^+ storage in TiO_2nts has not been studied yet. In this work, Li^+ storage in anatase TiO_2nts is investigated along side with the determination of the chemical diffusion coefficient for Li^+ insertion by electrochemical techniques, *i.e.* by cyclic voltammetry (CV) and chronoamperometry (CA), respectively.

Here, amorphous TiO_2nts were directly grown on Ti substrate by a simple anodization process, then they were annealed to form anatase phase which has a structure of body-centered tetragonal with the space group $I4_1/amd$. Fig. 1a shows the morphology of the crystalline TiO_2nts obtained by scanning electron microscopy (SEM). The cross-sectional view reveals the presence of highly-organized and smooth nanotubes with a length of 1.5 µm. Examination of the top view (inset) shows that the open diameter (100 nm) and the wall thickness (10 nm) are uniform.

The galvanostatic charge/discharge profiles of the anatase TiO_2nts in the half-cell using the gel polymer electrolyte and a Li foil as the reference are given in Fig. 1b. The TiO_2nt electrode was cycled at C/5 between 1.4 and 2.6 V *vs* Li/Li^+. The profiles show the discharge and charge plateaus at 1.75 and 1.9 V, respectively. Small plateaus observed in the discharge profile around 1.5V may result from the electropolymerization of the electrolyte. The electropolymerization stiffens the gel electrolyte, leading to decrease in ionic conductivity and capacity loss.[8,9] The cell delivers a reversible capacity of 35 µAh cm^{-2} or 140 mAh g^{-1} which is 83% of the theoretical capacity of the anatase TiO_2 (168 mAh g^{-1}). Unlike in the case of TiO_2 powder, self-supported TiO_2nts are directly grown on the Ti current collector, without mixing with any additives e.g. carbon black and polymer binder. Moreover, the gel electrolyte is in contact with TiO_2nts only on the tube tops. Thus, the accessibility of Li into the vacant sites in the lattice at the bottom of the tubes is limited only by the Li diffusion from the top. These factors may lower the capacity of TiO_2nts.

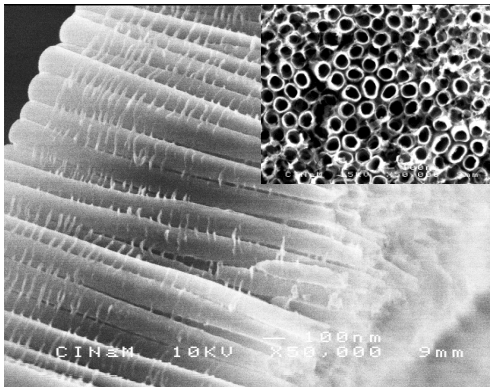

RSC Advances Accepted Manuscript

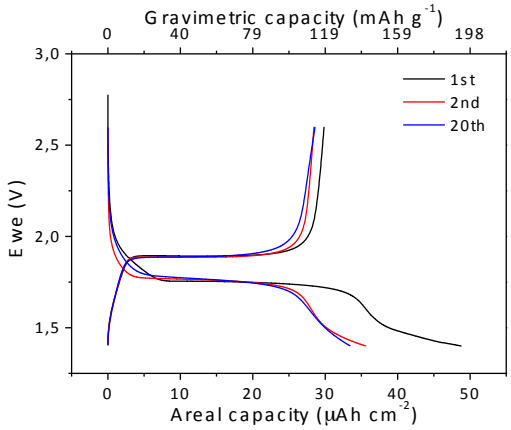

Fig. 1 (a) SEM images of TiO_2nts and (b) galvanostatic profiles of anatase TiO_2nt electrode in the half-cell using the polymer electrolyte and a Li foil as the reference.

The reversible insertion reaction of Li^+ in anatase TiO_2 is given by Eq. (1).

$$TiO_2 + xLi^+ + xe^- \rightleftharpoons Li_xTiO_2 \text{ for } 0 \le x \le 0.5 \qquad (1)$$

The Li^+ storage mechanism in TiO_2nts can be studied by varying the scan rates and recording the peak discharge currents. These data can be exploited to determine whether Li^+ is accommodated in the bulk lattice and/or at the surface of the nanotubes according to a pseudo-capacitive mechanism.

Fig. 2a shows five CV curves recorded in the potential window of 1.4 – 3.0V *vs* Li/Li^+ at different scan rates (0.05 – 0.8 mV s^{-1}). The redox peaks are well defined. The Li^+ insertion (cathodic peak) and extraction (anodic peak) occur at 1.72 and 1.97 V *vs* Li/Li^+, respectively. The positions of the redox peaks are in agreement with the positions of the Li^+ insertion/extraction plateaus in the galvanostatic profiles observed in Fig. 1b. It can be seen that faster scan rate, the higher currents, the broader peaks, and the shift of the cathodic and anodic peaks to the lower and higher potential values, respectively. These phenomena result from the combination of kinetic and *iR* drop effects.[10–12]

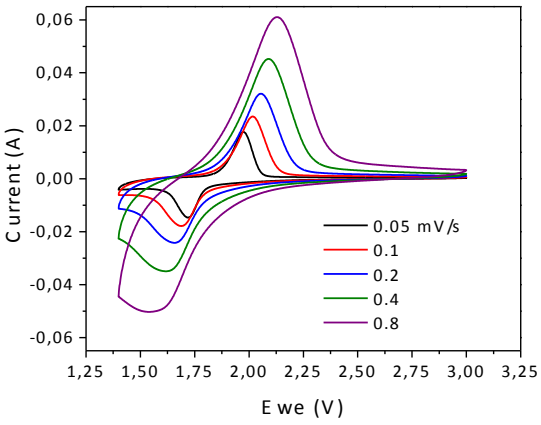

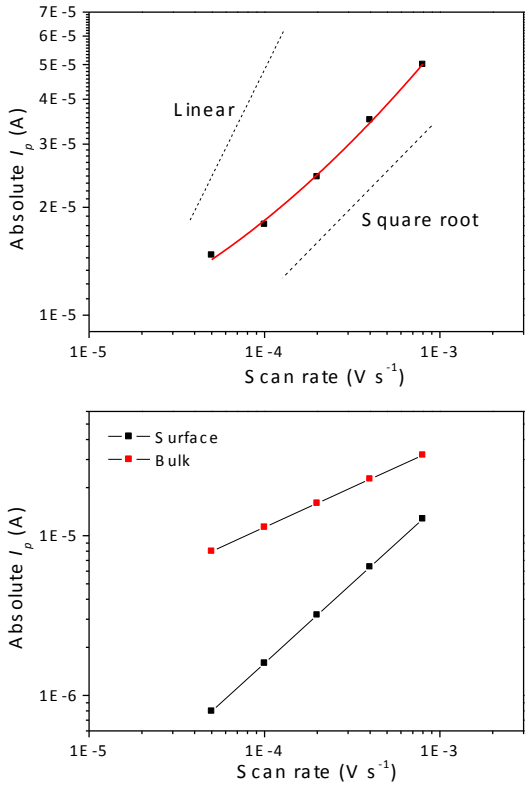

Fig. 2 (a) CV curves at different scan rates (■) experimental data, (—) fitting and (b) peak discharge current (I_p) versus scan rate plot: and (c) calculated I_c and I_d

Fig. 2b shows the peak discharge current (I_p) as a function of the scan rate (v). The best fit of the experimental data using an apparent power-law dependence give the apparent exponent value of 0.66 ($I_p \propto v^{0.66}$). Theoretically, the process of Li^+ storage can be obtained from Eq. (2) [13,14]

$$Ip = C_1v + C_2v^{1/2} \qquad (2)$$

Where the first term C_1v corresponds to the insertion of Li^+ at the surface leading to the pseudo-capacitive current (I_c) and the second term $C_2v^{1/2}$ is attributed to the bulk intercalation responsible for the faradic current (I_d). In the case of Li^+ storage occurring only in the bulk TiO_2, the exponent would be 0.5 while it is close to 1 when the pseudo-capacitive effect is predominant. Since the exponent is equal to 0.66, the Li^+ storage mechanism is governed by the bulk intercalation and the surface reaction processes. The fit of the experimental data with Eq. 2 corresponding to the solid red line in Fig. 2b gives $C_1 = 0.016 \pm 0.006$ and $C_2 = 0.0011 \pm 0.0002$. The upper and lower dash lines represent the linear (pure I_c) and square-root (pure I_d) dependence on the scan rate, respectively. These results reveal that the bulk intercalation of Li^+ in the interstitial sites of anatase is predominant although the storage of charges also occurs partially at the surface.

The mechanism of Li^+ insertion is also strongly dependent on the kinetics. Fig. 2c shows the variation of the calculated I_c (C_1v) and I_d ($C_2v^{1/2}$) *vs* the scan rate. At slow scan rate, I_d is predominant (for example at 0.05 mV s^{-1} the ratio $I_d : I_c$ is 10:1) suggesting that Li^+ are mainly accommodated in the bulk material. When the scan rate increases, I_c becomes more

RSC Advances Accepted Manuscript

This journal is © The Royal Society of Chemistry [year]

significant since the diffusion of Li^+ into the lattice is the rate limiting parameter. These results confirm that the pseudo-capacitive effect increases at fast kinetics.

The diffusion coefficient of Li^+ at room temperature of 25°C can be calculated using the Randles-Sevcik equation:

$$I_p = 268{,}600n^{3/2}AD^{1/2}Cv^{1/2} \quad (3)$$

where I_p is the peak current, n is the number of electrons involved in the redox reaction of Ti^{3+}/Ti^{4+} which is equal to 0.5 according to Eq. (1), F is the Faraday constant, A is the electrode surface area (active surface area of TiO_2nts) which is approximately 32 cm^2, D is the diffusion coefficient of Li^+, C is the maximum concentration of Li^+ (or Ti^{3+}) in the lattice (0.024 mol cm^{-3} at x=0.5).[14–16] According to Eq. (2), the term $268{,}600n^{3/2}AD^{1/2}C$ corresponds to C_2 = 0.0011. Therefore, the diffusion coefficient of Li^+ at room temperature is equal to 2.2 × 10^{-16} cm^2 s^{-1}.

Fig. 3 shows the chronoamperometric plot obtained by applying a constant potential of 1.7 V *vs* Li/Li^+, which is the potential insertion of Li^+ into the lattice. The variation of the current density recorded between the maximum value and the plateau can be described by the Cottrell equation given in Eq. (4):[16]

$$j = nFCD^{1/2}\pi^{-1/2}t^{-1/2} \quad (4)$$

The Cottrell equation is valid only in the diffusion control region (in our case approximately from few ms to 20 s). The diffusion coefficient can be estimated by plotting the absolute current density *vs* $t^{-1/2}$. Ideally, the plot is a linear straight line when the kinetic is controlled by mass transport. The value of the slope equal to $nFCD^{1/2}\pi^{-1/2}$ can be determined by the linear fit (solid red line). The calculated diffusion coefficient for Li^+ is estimated to be 2.1 × 10^{-16} cm^2 s^{-1} which is consistent with the result obtained from the CV experiments.

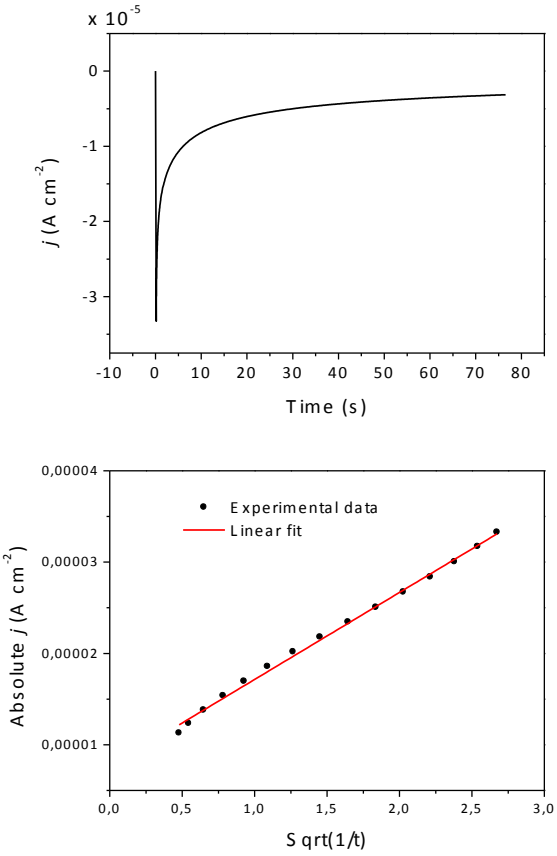

Fig. 3 (a) chronoamperometric plot and (b) Absolute current density (j) versus square-root (1/t): (●) experimental data, (–) linear fit.

The values obtained from our different experiments are very close to those reported by Lindström et al.[14,15] Indeed, the diffusion coefficient of Li^+ in nanoporous anatase TiO_2 studied in liquid electrolyte was found to be 2 × 10^{-17} cm^2 s^{-1} from the CV and 1 × 10^{-17} cm^2 s^{-1} from the CA. This result would indicate that one-dimensional nanomaterials such as vertical arrays of nanotubes can channel the migration of charges improving their transport even in solid electrolyte. However, it has to be noticed that the active surface area strongly influences the calculation. The actual active surface area and the projected area may give diffusion coefficients differing by several orders of magnitude.

Experimental Section

TiO_2nts were fabricated as reported in previous works.[6,8] The detailed procedure is provided in the supporting document. Briefly, a cleaned Ti foil was electrochemically anodized in a glycerol electrolyte containing 2 %wt. water and 1.3 %wt. NH_4F. A constant voltage of 60V was applied to the electrochemical cell usig Ti foil as the working electrode and Pt foil as the counter electrode for 3h. Anatase TiO_2nts was obtained by annealing the as-formed TiO_2nts at 450°C under air atmosphere for 3h. The half-cells were consisting of TiO_2nt layer assembled against a metallic Li foil using two-electrode Swagelok test cells. Two circular sheets (diameter of 10 mm) of separator were placed

RSC Advances Accepted Manuscript

between the two electrodes. The separator was prepared by soaking the Whatman glass microfiber with an aqueous solution of 0.5M LiTFSI + 0.5M poly(ethylene glycol) methyl ether methacrylate (MA-PEG500) with the average molecular weight of 500 g mol^{-1}. The gel electrolyte embedded in the Whatman paper was obtained after drying the separator in the BUCHI vacuum dryer at 60 °C overnight. The galvanostatic experiments were performed at C/5 in the potential window of 1.4 – 2.6 V *vs* Li/Li^+. The CV experiments were conducted at various scan rates (0.05 – 0.8 mV s^{-1}) in the potential between 1.4 and 3.0 V *vs* Li/Li^+. The CA was studied in a three-electrode Swagelok cell. TiO_2nt electrode was assembled against one Li foil serving as a counter electrode and another Li foil as a reference electrode. Two separators were placed between each electrode. The CA test was performed by applying a constant potential of 1.7 V during 80 s. All the electrochemical measurements were performed using a VMP3 potentiostat-galvanostat (Bio Logic).

Conclusions

We have investigated the Li^+ storage mechanism at room temperature in the anatase TiO_2nts using a gel polymer electrolyte (LiTFSI dissolved in MA-PEG500). It is found that the Li^+ storage is governed by intercalation of Li^+ into the bulk with a pseudo-capacitive contribution even at low kinetics. The chemical diffusion coefficient of Li^+ in TiO_2nts at room temperature is around 2×10^{-16} cm^2 s^{-1} estimated from the CV and the CA. These values obtained from two different techniques suggest that self-organized titania nanotubes tested in polymer electrolyte can still promote diffusion of charges.

Acknowledgements

This work has been carried out thanks to the support of the A*MIDEX project (*n° ANR-11-IDEX-0001-02*) funded by the "Investissements d'Avenir" French government program, managed by the French National Research Agency (ANR). We also acknowledge ANR JCJC no.2010 910 01.

Notes and references

[a] *Aix-Marseille University, CNRS, MADIREL UMR 7246, F-13397, Marseille, Cedex 20, France*
[b] *FR CNRS 3459, Réseau sur le Stockage Electrochimique de l'Energie (RS2E), Paris, France*
[c] *FR CNRS 3104, ALISTORE-ERI, France*

1 B. L. Ellis, P. Knauth and T. Djenizian, *Adv. Mater.*, 2014, **26**, 3368–3397.

2 P. G. Bruce and C. A. Vincent, 1993, **89**, 3187–3203.

3 R. C. Agrawal and G. P. Pandey, *J. Phys. D. Appl. Phys.*, 2008, **41**, 223001.

4 Q. Xiao, X. Wang, W. Li, Z. Li, T. Zhang and H. Zhang, *J. Memb. Sci.*, 2009, **334**, 117–122.

5 R. Bernhard, A. Latini, S. Panero, B. Scrosati and J. Hassoun, *J. Power Sources*, 2013, **226**, 329–333.

6 N. Plylahan, S. Maria, T. N. T. Phan, M. Letiche, H. Martinez, C. Courrèges, P. Knauth and T. Djenizian, *Nanoscale Res. Lett.*, 2014, **9**, 544.

7 N. Plylahan, M. Letiche, M. K. S. M. K. S. Barr and T. Djenizian, *Electrochem. Commun.*, 2014, **43**, 121–124.

8 N. Plylahan, M. Letiche, M. Kenza, S. Barr, B. Ellis, T. N. T. Phan, E. Bloch and P. Knauth, *J. Power Sources*, 2015, **273**, 1182–1188.

9 N. A. Kyerematen, F. Dumur, P. Knauth, B. Pecquenard and T. Djenizian, *Electrochem. Commun.*, 2011, **13**, 894–897.

10 W. Wei, G. Oltean, C.-W. Tai, K. Edström, F. Björefors and L. Nyholm, *J. Mater. Chem. A*, 2013, **1**, 8160.

11 A. J. Bard and L. R. Faulkner, *Electrochemical Methods*, Wiley, New York, 2nd edn., 2001.

12 P. L. Taberna, S. Mitra, P. Poizot, P. Simon and J. M. Tarascon, *Nat. Mater.*, 2006, **5**, 567.

13 K. Zhu, Q. Wang, J. Kim, A. A. Pesaran and A. J. Frank, *J. Phys. Chem. C*, 2012, **116**, 11895–11899.

14 H. Lindström, S. Södergren, A. Solbrand, H. Rensmo, J. Hjelm, A. Hagfeldt and S. Lindquist, *J. Phys. Chem. B*, 1997, **101**, 7717–7722.

15 H. Lindström, S. Södergren, A. Solbrand, H. Rensmo, J. Hjelm, A. Hagfeldt and S. Lindquist, *J. Phys. Chem. B*, 1997, **101**, 7710–7716.

16 L. Kavan, M. Grätzel, S. E. Gilbert, C. Klemenz and H. J. Scheel, *J. Am. Chem. Soc.*, 1996, **118**, 6716–6723.

RSC Advances Accepted Manuscript

This journal is © The Royal Society of Chemistry [year]